

## Research Article

# Mix and Inject: Reaction Initiation by Diffusion for Time-Resolved Macromolecular Crystallography

**Marius Schmidt**

*Physics Department, University of Wisconsin-Milwaukee, WI, USA*

Correspondence should be addressed to Marius Schmidt; [m-schmidt@uwm.edu](mailto:m-schmidt@uwm.edu)

Received 27 December 2012; Accepted 8 April 2013

Academic Editor: Abbas Ourmazd

Copyright © 2013 Marius Schmidt. This is an open access article distributed under the Creative Commons Attribution License, which permits unrestricted use, distribution, and reproduction in any medium, provided the original work is properly cited.

Time-resolved macromolecular crystallography unifies structure determination with chemical kinetics, since the structures of transient states and chemical and kinetic mechanisms can be determined simultaneously from the same data. To start a reaction in an enzyme, typically, an initially inactive substrate present in the crystal is activated. This has particular disadvantages that are circumvented when active substrate is directly provided by diffusion. However, then it is prohibitive to use macroscopic crystals because diffusion times become too long. With small micro- and nanocrystals diffusion times are adequately short for most enzymes and the reaction can be swiftly initiated. We demonstrate here that a time-resolved crystallographic experiment becomes feasible by mixing substrate with enzyme nanocrystals which are subsequently injected into the X-ray beam of a pulsed X-ray source.

## 1. Enzymology

The “unspent vital force” was the historical and metaphysical expression for a biological catalyst. It was eradicated in 1890 by an article worth almost 100 pages by O’Sullivan and Tompson [1], which probably denotes the beginning of what we know now as enzymology. The enzyme was originally thought to be the leaven in sour dough and then materialized as a chemical, a macromolecule, or something that can be manipulated, tested, and investigated. Similarities with chemical catalysts were discovered. This finally led to the nowadays well-established and important field of enzymology. In 1926 Sumner reported the purification and crystallization of the first enzyme, urease [2]. At that time, X-ray structure determination has been established starting in the first decade of the 20th century. Although the father of X-ray crystallography, Max von Laue, did not believe that it would be possible to determine atomic structures of enzymes with X-ray crystallography [3], the first structures of proteins were determined at the end of the 50s and the beginning of the 60s of the last century [4, 5]. Only then biologists learned to think in terms of 3D atomic structure of biological molecules. Structure-function relationships were discovered. Enzymes could be studied by directly seeing how, where, and in which orientation effectors were binding to the enzyme. Phenomena

such as allosteric inhibition of enzyme activity first discovered by enzyme kineticists finally could be understood on the atomic length scale. This provided new venues, for example, to design new drugs to cure diseases. However, the atomic structures were still static. Enzymologists knew that catalysis must be accompanied by structural transitions of the catalyst. At thermal equilibrium, in crystallography, conformational heterogeneity and structural fluctuations are hidden in the Debye-Waller factor [6]. The protein is flexible, even in the crystal. Catalytic function, structural flexibility, and heterogeneity are intimately related. Once the atomic structure is locked into place, the enzyme is dead and nonfunctional [7]. However, in most cases protein crystals are catalytically active and the crystalline lattice does not constrain the dynamics of the enzyme that would otherwise impair its function. At the end of the 20th century, crystallography evolved to the point that the catalytic action of proteins could be observed directly in the crystal. Time-resolved crystallography made this possible [8, 9]. Ultrafast time-resolved crystallography is a pump-probe method that requires short, extremely intense X-ray pulses to achieve the best time resolution. Snapshots of a protein in action in the crystal can be taken as a function of time after the reaction is initiated and assembled into a movie. This movie shows how the protein ensemble evolves in the crystal. The crystallographic experiment becomes a kinetic

experiment. The rise and decay of short lived (transient) states can be observed during the reaction. Since it is a crystallographic experiment, the structures of the transient states can be determined from the same data. Chemical, kinetic mechanisms that connect the states can be tested and become falsifiable [10–12]. Each new transient state structure is biologically interesting and may be a new drug target. It can be manipulated to alter the chemical, kinetic mechanism of a specific reaction with the goal, for example, to bring that reaction to a full stop in order to eradicate a pathogen.

## 2. The Challenge

The long-term goal is to rapidly and routinely investigate all kinds of biologically and pharmaceutically interesting enzymatic reactions with time-resolved crystallography. There are limitations that prevented the maturation of this technology to its full potential so far. The three most prominent ones are (i) the limited pulse intensity at the synchrotron, (ii) limited crystal quality, and (iii) the necessity to mount single crystals for exposure to the X-rays. Whereas the former (i) allows for improvements, for example, by microfocusing to reach single pulse capability even with small crystals, the latter two are by far the most challenging of all, and there is no satisfactory solution for this to date. When a single crystal is mounted, typically in a capillary for room temperature studies, it can be exposed many times to the X-ray pulses. The structure can be solved by rotating the crystal to collect the integrated reflection intensities. However, rotation is almost always prohibitive with fast reactions, simply because the crystal cannot be rotated fast enough through the Ewald sphere. One way out is the usage of the Laue method where a bandwidth of X-rays is used to collect the intensities from stills. With the Laue method one needs good crystals with low mosaicities. Otherwise the reflections become too streaky and their intensities cannot be extracted [13, 14]. Poor crystal quality, which might potentially get worse when the reaction proceeds, already excludes many, otherwise interesting enzymes. If an enzymatic reaction is to be investigated, the reaction can be initiated only once in a particular volume of the crystal, because it is typically noncyclic or irreversible. With fast detectors the reaction might be followed up using subsequent X-ray exposures and readout between the pulses. Readout times of large area detectors are constantly improving [15–17] with the goal of MHz (!) readout rates. However, when the reaction is over, the product must be removed, new substrate loaded and the crystal reset to cover more of reciprocal space to assemble a complete dataset. This can be achieved by either probing another, previously unaffected crystal volume, by using flow cells [18] to wash away product and load new substrate, or by mounting another crystal charged with substrate all together. The latter two methods are tedious and prevent rapid results. For cyclic reactions such as dissociation and geminate rebinding reactions in heme proteins the situation is different. One waits until the reaction comes to an end, resets the crystal, reinitiates the reaction, and repeats the experiment until radiation damage is so severe that either the crystal is destroyed or the kinetics are altered, whichever comes

first [19]. These are the reasons that so few reactions that were investigated by time-resolved crystallography are actually enzymatic reactions. Most of them are cyclic reactions in heme proteins and light activated signaling proteins [20–30]. Nevertheless, lessons learned from these experiments are priceless. Structural relaxations become directly accessible and transient state structures explain a vast number of results previously taken by spectroscopic approaches. Most importantly, chemical kinetics are united with structure determination, something that the early crystallographers would not have believed in their wildest dreams. However, approaches to enzymatic reactions remain sparse [31–34]. To change this, it will be shown in the following that any X-ray source can be used that provides enough flux into single ultrashort pulses to probe tiny crystals so that the time-resolved experiments do not depend on the availability of large crystals. In particular, new generation X-ray sources, XFELs, provide sufficient flux and are monochromatic, and pulses are short enough that diffraction patterns become insensitive to radiation damage.

## 3. Nanocrystallography at XFEL

The 4th generation X-ray sources deliver on the order of  $10^{12}$  photons in a single femtosecond, monochromatic X-ray pulse. Since the pulses are so short, diffraction occurs before the specimen is destroyed. Accordingly, the diffraction patterns are free of radiation damage. In addition, the conventional rotation method can be given up in favor of injecting small crystals directly into the beam. During the femtosecond pulse duration all motions of the crystal are frozen in time. One obtains a snapshot of the crystal akin to a still exposure, but with the crystal in random orientation. It has been shown recently that a complete data set with sufficient resolution can be collected by injecting a large number of these small, randomly oriented crystals [35]. Data reduction differs from the conventional rotation method in so far that a large number ( $>100,000$ ) of randomly oriented diffraction patterns containing only partial reflections are available from which the integrated reflection intensities must be reconstructed [36]. Due to its enormous spatial coherence, the XFEL beam can be focused on a nanometer sized focal spot. In this case crystals with edge length on the order of nanometers can be injected into the beam and yield analyzable diffraction patterns. This allows structure determination even from crystals naturally grown within cells [37, 38]. This technology has been named “serial femtosecond X-ray crystallography” (SFX) [39].

A time-resolved crystallographic experiment may benefit from these ultrashort pulses [40], provided the reaction itself can be initiated on a similar time scale. In these cases the ultimate time resolution given by the X-ray pulse can potentially be reached. Typical examples include the mentioned photoflash experiments on heme proteins, where a small molecule such as carbon monoxide can be flashed away from the heme moiety by an ultra-short laser pulse. With enzymes, however, it is exceptionally difficult to initiate a reaction on this ultrashort time scale. The reason for this is that substrate would have to be provided to the enzyme in an ultrafast

fashion. This turns out to be very difficult if not impossible to do on the sub- $\mu\text{s}$  time scale. In an ideal case, inactive, so-called caged substrate is soaked into the crystals and binds directly to the active center. Then diffusion times are extremely short. The caged substrate is activated by a short laser pulse. Typical activation rates vary widely from nanoseconds to milliseconds [41, 42]. Chemical expertise is necessary to design and produce new caged substances tailored to the reaction to be investigated, which, in many cases, are not routinely available. Also, the quantum yield for activation is typically low and a single laser shot might not be sufficient to activate a significant fraction of the caged substrate. Cryophotolysis combined with temperature-controlled freeze-trap cycles can be used to trap intermediates even in the fastest enzymes [43]. Still, the ultimate goal is to let the reaction in an enzyme advance freely and at ambient temperatures. A number of such experiments were conducted at the synchrotron with the Laue method to date [31, 34, 44–48]. An enzyme that crystallizes excellently as well as a caged substrate whose activation time complies with the time-resolution is required. For routine applications it is highly desirable that the reaction is initiated in a different way than using a sample-specific caged substrate. The simplest way is to mix crystals and active substrate and let the substrate diffuse into the crystal. Once substrate is present at the active site, the reaction starts. Assuming that crystals can be mixed with substrate fast enough, objections to this approach are causally connected: (i) time resolution would depend on diffusion times and (ii) zero time, the point in time where the reaction starts, would be dependent on the position in the crystal. Both objections are void, if diffusion times are much faster than the characteristic lifetimes of the intermediates to be investigated. We will explore this possibility further in the following sections. With methods of linear algebra such as singular value decomposition the time information can be exploited in a sense that it might be possible to correct for the zero time distribution and push time resolution to the limit.

#### 4. Velocities in Enzymes and the ccNIR Reaction

Reaction times in enzymes vary enormously. The fastest enzyme is probably the catalase [49] with catalytic rates  $k_{\text{cat}}$  on the order of  $10^6$ . The turnover time is  $1/k_{\text{cat}}$  on the order of a microsecond. Other enzymes such as the hydroxymethylbilane synthetase react on the order of hours [50]. Most other enzymes are lying in between with catalytic rates of 100 1/s or so [51]. This means that at least millisecond time resolution is required to characterize these reactions adequately. In Figure 1 the reaction catalyzed by the enzyme cytochrome-c nitrite reductase (ccNIR) is shown as an example. This enzyme is one of the most important enzymes in the biologically highly relevant nitrogen cycle and reduces nitrite to ammonia in a 6-electron transfer reaction. Three intermediates are formed during the catalytic cycle. These are the ccNIR-nitric oxide, the ccNIR-hydroxylamine, and finally the ccNIR-ammonia complexes, all structures of which are unknown due to the short lifetimes of the corresponding transient states. Recently,

we determined the structure of the ccNIR of *Shewanella oneidensis* [52]. Its turnover time at room temperature is about 1.2 ms ( $k_{\text{cat}} = 824$  1/s). Several intermediates accumulate during the reaction. A transient state experiment needs a time resolution that is on the submillisecond time scale.

The ccNIR of *S. oneidensis* is difficult to work with. Crystals are labile and sensitive to radiation damage. After about 10 monochromatic X-ray exposures, the diffraction patterns fade away. A time-resolved crystallographic experiment on this ccNIR is very challenging. It requires great chemical expertise to produce suitable electron donors attached to the ccNIR in the crystal that can be activated by short laser flashes for the reaction to proceed in a time-resolved fashion. These experiments are underway. However, the following proposes time-resolved crystallographic experiments where chemical expertise is kept at a minimum, the extent of reaction initiation is large, the crystal quality can be moderate, radiation damage is zero, and time resolution is good enough to capture the reaction intermediates. This experiment has the potential to transform enzymology because it produces entire time series (movies) from reactions in enzymes rapidly. Most importantly it has the potential to become a routine procedure to investigate all kinds of enzymatic reactions. The requirement is that micro and nanocrystals can be obtained from the enzyme and that the substrate is soluble, which is true for most enzymes.

#### 5. “Mix and Inject” at a Pulsed X-Ray Source

The traditional approach to enzymology is to mix enzyme with substrate and follow the reaction with time-resolved methods such as time-resolved absorption spectroscopy. For this, special devices are constructed called either continuous-flow or stopped-flow devices [51]. The enzyme is mixed with substrate and injected into a cuvette. The evolution of the mixture in the cuvette is probed, for example, with visible light. Newer mixing devices allow time resolutions as good as about 150  $\mu\text{s}$  [53]. The design of the mixer must be modified to be used for time-resolved crystallography in order to inject nano- and microcrystals into the X-ray beam (Figure 2(a)). The goal is to control both mixing and injecting and synchronize it with the arrival time of the ultrashort X-ray pulse. The time delay  $\Delta t$  could be selected by either controlling the residence time of crystal and substrate in the mixer or by varying the distance  $\Delta L$  of the mixer from the pulsed X-ray beam given the velocity of the ejected droplet. Consequently, injector technology is a key to this experiment. Injector technology to deliver specimen into the XFEL beam progressed rapidly in the last few years [54–57]. However, a device that performs both mixing and synchronized injection is needed. A prerequisite to the success of this method is that not only mixing can be performed rapidly, but also diffusion times into the crystals are kept at a minimum. If diffusion times are longer than the turnover time of the enzyme, the time resolution becomes so poor that it would be impossible to conduct a transient state kinetic experiment.

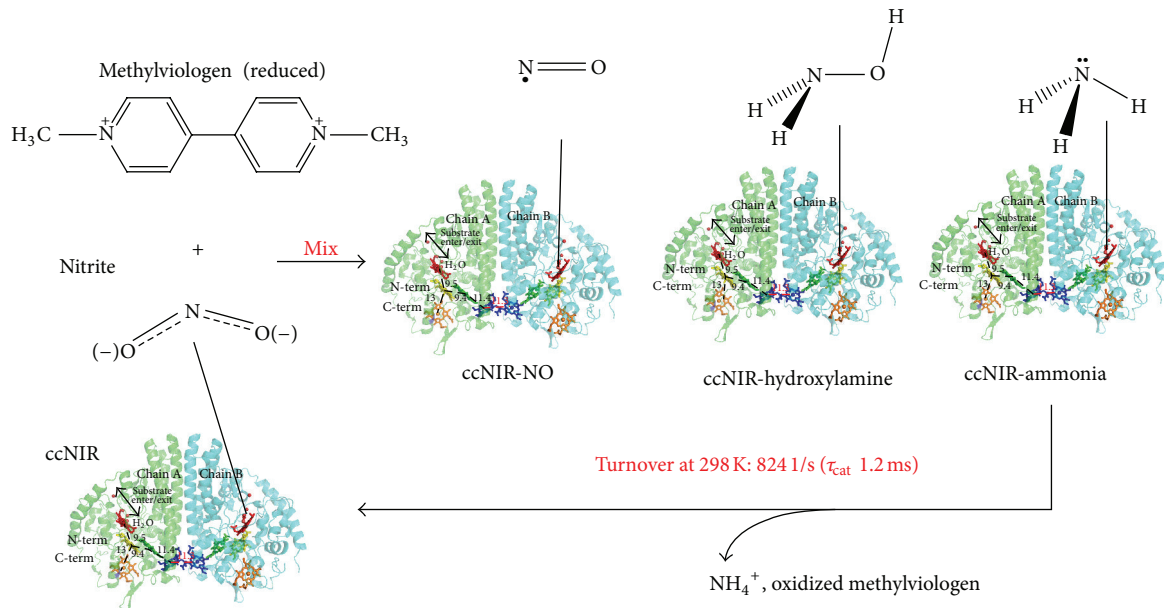


FIGURE 1: Catalytic cycle of the ccNIR. Initially, nitrite binds to a specific c-heme in the ccNIR. Methylviologen serves as electron donor for the 6-electron transfer reaction to produce ammonia from nitrite. The NO, hydroxylamine, and ammonia complexes are shown. The catalytic rate is 824 1/s at room temperature.

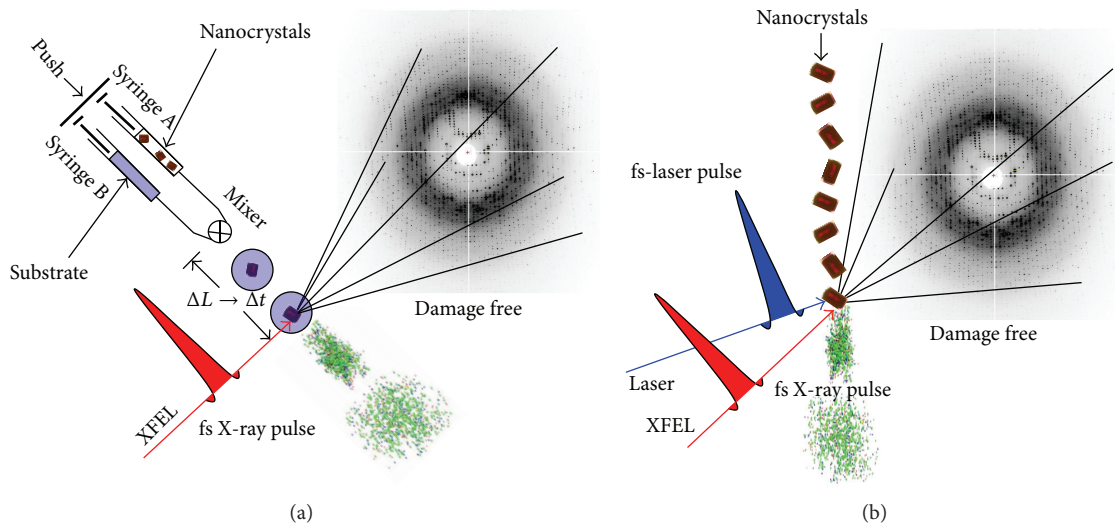


FIGURE 2: (a) Schematic setup for a mix and inject time-resolved femtosecond serial crystallographic experiment at the XFEL. Nano- and microcrystals are in syringe A and substrate in syringe B. After mixing, the crystal/substrate droplet is injected into the XFEL beam. The crystal might disintegrate after the fs X-ray pulse, but diffraction occurs earlier. The diffraction pattern is damage free. (b) Time-resolved pump-probe experiment with serial femtosecond crystallography. Setup can be used to stimulate photoreceptors for photoflash experiments or to activate caged substrates. Conceptual similarities between (a) and (b) are obvious.

## 6. Diffusion Times

Diffusion of (a soluble) substrate in solution follows Fick's 2nd law (1),

$$D\nabla^2 c = \frac{\partial c}{\partial t}, \quad (1)$$

where  $D$  is the diffusion coefficient, and  $\nabla^2$  is the Laplace operator,  $c$  is the time-dependent concentration of the diffusing species. Equation (1) is a second order partial differential equation that can be solved by separation of variables. In special cases an analytic solution can be found subject to certain boundary conditions. In most other cases solutions are only

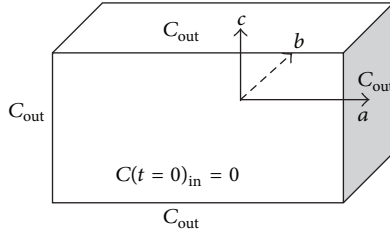


FIGURE 3: Shoe-box like crystal with sides  $2a$ ,  $2b$ , and  $2c$ . The substrate concentration is  $C_{\text{out}}$  outside the crystal at any time. Inside,  $C_{\text{in}}$  is initially zero and evolves as a function of time.

found by numerical methods. The simple case of substrate diffusing into a shoe-box like crystal with sides  $2a$ ,  $2b$ , and  $2c$  is depicted in Figure 3. The situation is idealized by assuming the following: (i) the change of the outside concentration of the substrate is negligible at all times, (ii) binding of substrate to the enzyme is neglected, so that the substrate diffuses freely into the crystal, and (iii) mixing of crystal with substrate is instantaneous at time  $t = 0$ , so that the concentrations  $c$  of the substrate inside and outside are  $C_{\text{out}} = C$ , so that the concentration of substrate outside the crystal is  $C_{\text{out}}$  and the concentration  $C$  inside is zero initially. With these boundary conditions, the solution to Fick's 2nd law is (2) [58]:

$$\begin{aligned}
 C(x, y, z, t) &= C_{\text{out}} \left[ 1 - \frac{64}{\pi^3} \sum_{l=0}^{\infty} \sum_{m=0}^{\infty} \sum_{n=0}^{\infty} \frac{(-1)^{l+m+n}}{(2l+1)(2m+1)(2n+1)} \right. \\
 &\quad \times \cos \frac{(2l+1)\pi x}{2a} \cos \frac{(2m+1)\pi y}{2b} \\
 &\quad \times \cos \frac{(2n+1)\pi z}{2c} \\
 &\quad \left. \times \exp^{-\frac{D\pi^2}{4} \left[ \frac{(2l+1)^2}{a^2} + \frac{(2m+1)^2}{b^2} + \frac{(2n+1)^2}{c^2} \right] t} \right]. \quad (2)
 \end{aligned}$$

Equation (2) is reminiscent of a Fourier sum. The concentration of substrate inside the crystal is dependent on the initial outside concentration  $C_{\text{out}}$  and a time-dependent exponential term that contains the characteristic time scale  $\tau_D$  of the diffusion problem (3):

$$\tau_D = \frac{4}{D\pi^2 \left[ \frac{(2l+1)^2}{a^2} + \frac{(2m+1)^2}{b^2} + \frac{(2n+1)^2}{c^2} \right]}, \quad (3)$$

where  $\tau_D$  contains the diffusion coefficient  $D$  and accounts for the time after which the concentration of substrate reached  $1 - 1/e = 0.63$  of the initial amplitude of the corresponding Fourier term. The slowest  $\tau_D$  is that of the  $l, m, n = 0$  term, and everything else is faster. The  $l, m, n = 0$  term accounts for  $64/3\pi^3 = 69\%$  of the initial concentration. Consequently, this term accounts for almost all the concentration. The corresponding  $\tau_D$  is the slow limit for the diffusion time. Most

TABLE 1: Diffusion times  $\tau_D$  for various crystal sizes from calculation, simulation, and experiment.

| Crystal size   | $\tau_D$          |
|--|-------------------|
|  | 16 s (3)          |
| $400 \times 400 \times 1600 \mu\text{m}^3$             | 24 s [60]         |
|  | <1 min [59]       |
| $300 \times 400 \times 500 \mu\text{m}^3$              | 9.5 s             |
| $10 \times 20 \times 30 \mu\text{m}^3$                 | 15 ms             |
| $3 \times 4 \times 5 \mu\text{m}^3$                    | 1 ms              |
| <sup>a</sup> $1 \times 2 \times 3 \mu\text{m}^3$       | 150 $\mu\text{s}$ |
| $0.5 \times 0.5 \times 0.5 \mu\text{m}^3$              | 17 $\mu\text{s}$  |
| <sup>b</sup> $0.1 \times 0.2 \times 0.3 \mu\text{m}^3$ | 1.5 $\mu\text{s}$ |

<sup>a</sup>With much smaller crystals mixing times might be slower than diffusion times.

<sup>b</sup>*S. oneidensis* ccNIR crystals would have about 4000 unit cells.

importantly,  $\tau_D$  depends on the square of the crystal half sides  $a$ ,  $b$ , and  $c$ . This is apprehensible, since diffusion into a volume is dependent on the surface exposed. Equation (3) is used to calculate the evolution of substrate concentration in the center of the crystal at  $x, y, z = 0$  (see Table 1) using the diffusion coefficient  $D = 5 \times 10^{-6} \text{ cm}^2/\text{s}$  for a typical substrate, glucose, previously measured in a crystal [59]. Results are compared to those obtained from numerical simulation and experiment. Table 1 shows that diffusion times into macroscopic crystals are on the order of 20 s, as found from our simple equation and by a more complex and accurate numerical simulation [60], which has been corroborated by a crystallographic experiment [59]. This shows that our calculation is in the right ballpark, and we can use it to determine diffusion times with various crystal sizes. If the crystal size shrinks by one order of magnitude, diffusion times accelerate by 2 orders of magnitude according to (3). Diffusion times into a  $3 \times 4 \times 5 \mu\text{m}^3$  crystal are already in the fast millisecond time regime (1 ms). For a  $1 \times 2 \times 3 \mu\text{m}^3$  crystal diffusion times become submillisecond (150  $\mu\text{s}$ ). This would be sufficient to initiate a time-resolved crystallographic experiment with the ccNIR. With lysozyme atomic structures were already successfully determined from crystals of similar sizes using fs X-ray pulses from the LCLS [35], and even smaller crystals can be used [61]. With  $0.5 \times 0.5 \times 0.5 \mu\text{m}^3$  nanocrystals diffusion times would approximately match the fastest mixing times, which is excellent for almost all reactions in biological macromolecules.

## 7. Simulations

In a time-resolved experiment, intermediate states can only be observed if they are populated sufficiently by active enzyme molecules. The concentrations of the intermediates are determined by the magnitudes of rate coefficients of the underlying chemical, kinetic mechanism. It is the goal of any time-resolved experiment to determine (i) the physical properties, for example, the atomic structures or the spectra, of the intermediate states, (ii) the time-dependent concentrations of these intermediates, and (iii) the magnitudes of all rate coefficients that specify the chemical, kinetic

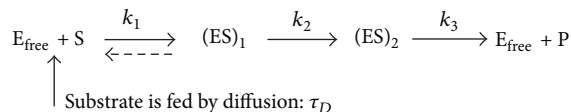


FIGURE 4: Chemical kinetic mechanism of a hypothetical enzymatic reaction where substrate is fed by diffusion. Two transient states, enzyme-substrate complexes  $(ES)_1$  and  $(ES)_2$  are successively populated until the free enzyme is released. The dashed arrow denotes a potential equilibrium that is ignored here.

mechanism of the reaction. To illustrate this, a chemical, kinetic mechanism is depicted in Figure 4 that features the free enzyme and 2 intermediate states. Given the magnitude of the rate coefficients in this mechanism, one can now assess how fast diffusion of substrate  $S$  into the crystal has to be that both intermediates are well separated in time. Only then can the time information be exploited to assess mixtures, separate these mixtures into pure states, and ultimately determine the structures of the pure, admixture-free intermediates from the time-resolved crystallographic data. Rate coefficient  $k_1$  in the mechanism is a second order rate coefficient that accounts for substrate binding to form enzyme-substrate complex 1  $(ES)_1$ .  $k_2$  and  $k_3$  are catalytic rate coefficients for conversion from  $(ES)_1$  to  $(ES)_2$  and finally to product  $P$  and free enzyme, respectively. The free enzyme can reenter the catalytic cycle at any time. Since  $k_1$  is a second order rate coefficient the rate itself depends sensibly on both, the concentration of free enzyme and the concentration of substrate. The magnitude of  $k_1 = 1000 \text{ L mmol}^{-1} \text{ s}^{-1}$  accounts for tight substrate binding. The other two rate coefficients are single step, first-order rate coefficients. From the value of  $4000 \text{ 1/s}$  for  $k_2$  one expects that  $(ES)_1$  decays on a  $1/4000 \text{ s} = 250 \mu\text{s}$  time scale.  $k_3$  is much smaller and is the rate limiting step of the enzyme.  $k_3$  is chosen ( $800 \text{ 1/s}$ ) that it matches approximately the catalytic rate of the ccNIR (see above). It is also assumed that the supply of substrate is constant at  $c_0 = 50 \text{ mmol/L}$ . Concentrations of proteins in crystals are up to  $100 \text{ mmol/L}$ . The concentration of the ccNIR is about  $25 \text{ mmol/L}$ , which is chosen here for the simulation. The characteristic diffusion time  $\tau_D$  is varied by changing the crystal size. For simplicity, the concentration of substrate at the center of the crystal is calculated from  $c(t) = c_0(1 - e^{-(1/\tau_D)(t)})$  with  $\tau_D$  given by (3) with  $l, m, n = 0$  and the diffusion coefficient of glucose in the crystal mentioned above.  $c(t)$  is fed to the free enzyme to start the reaction. A certain time after reaction initiation a steady-state must emerge in the simulations, because the assumption is that  $C_{\text{out}}$  is constant in time. The rate equations are coupled differential equations, which were solved for the concentrations of the particular intermediates and the free enzyme by numerical methods. Figure 5 shows the result.

Although the simulations are quite simple, the results are illuminating. In Figure 5(a) the reaction initiation is much faster than the turnover time, it is even faster than the binding rate to the free enzyme. This is an ideal case, which requires a caged substrate that can be quickly activated. Free enzyme and the enzyme-substrate complexes  $(ES)_1$  and  $(ES)_2$  are well separated in time. The steady state forms after one

turnover. It consists of 83%  $(ES)_2$  which is contaminated by a small amount (17%) of  $(ES)_1$ . The structures of the pure intermediates in conjunction with a suitable chemical, kinetic mechanism are likely to be extractable from time-resolved crystallographic movie using established methods [11]. In Figure 5(b), diffusion times are comparable to the turnover time. The concentration profiles for free enzyme,  $(ES)_1$  and  $(ES)_2$ , do not differ very much from those in Figure 5(a). This is because only a very little substrate concentration is necessary to bind to the free enzyme. However, the free enzyme is pulled down later (see vertical dashed lines), which is still faster than the turnover time.  $(ES)_1$  accumulates properly. As long as the conditions are such that sufficient  $(ES)_1$  accumulates before it decays to  $(ES)_2$ , the intermediates are separable. Again the steady state forms, when changes in the substrate or the free enzyme concentrations are negligible. When diffusion times are much longer than the turnover time (Figure 5(c)), it is not possible to use the time information to separate the intermediates. Formation of  $(ES)_1$  is on the same time scale than  $(ES)_2$  because the velocity (rate) of the formation of  $(ES)_1$  depends on both substrate and free enzyme. The substrate concentration, however, is very small up to 100 ms. At the same time  $(ES)_1$  is already decaying, and the ratio  $(ES)_1/(ES)_2$  is roughly given by  $k_3/k_2$  at any time. The steady state is delayed (dashed blue arrow) until the free enzyme concentration is negligible or the substrate reaches a constant level. In all instances, probing the steady state is possible even with conventional monochromatic crystallography. No or very little time-resolution is required. Under steady state conditions the Michaelis complex, which is here a mixture of  $(ES)_2$  and  $(ES)_1$ , can be extracted from the crystallographic data. This is already very valuable information for the enzymologist. The simulations show that for transient state experiments where  $(ES)_1$  and  $(ES)_2$  states are well separated in time, small crystals must be used. A size of  $3 \times 4 \times 5 \mu\text{m}^3$  is sufficient (Figure 5(b)) whereas the experiment likely fails with crystals that are an order of magnitude larger. Of course, all of this depends on, in addition to the magnitude of the rate coefficients in the kinetic mechanism, the diffusion coefficient of the substrate in the crystal and the highest substrate concentration  $C_{\text{out}}$  that can be prepared and used under the experimental conditions.

## 8. Discussion

Figure 2 shows that cyclic (reversible) and noncyclic (non-reversible) reactions as well as mix and inject and pump-probe experiments are on the same footing. With somewhat larger crystals and correspondingly lower time resolution, mix and inject experiments are already at the reach of the synchrotron. Time resolutions on the order of 5 ms could be achieved with  $10 \mu\text{m}$  sized crystals which would easily tolerate the dose deposited by the 100 ps long synchrotron X-ray pulse [62], and “diffract before destroy” would not be necessary. However, the single pulse capability of the X-ray source mentioned earlier is required. The best time-resolution can only be achieved with the smallest crystals and an XFEL is required. If these crystals are hit by the XFEL beam, they are destroyed. Doses absorbed [35] are several orders of

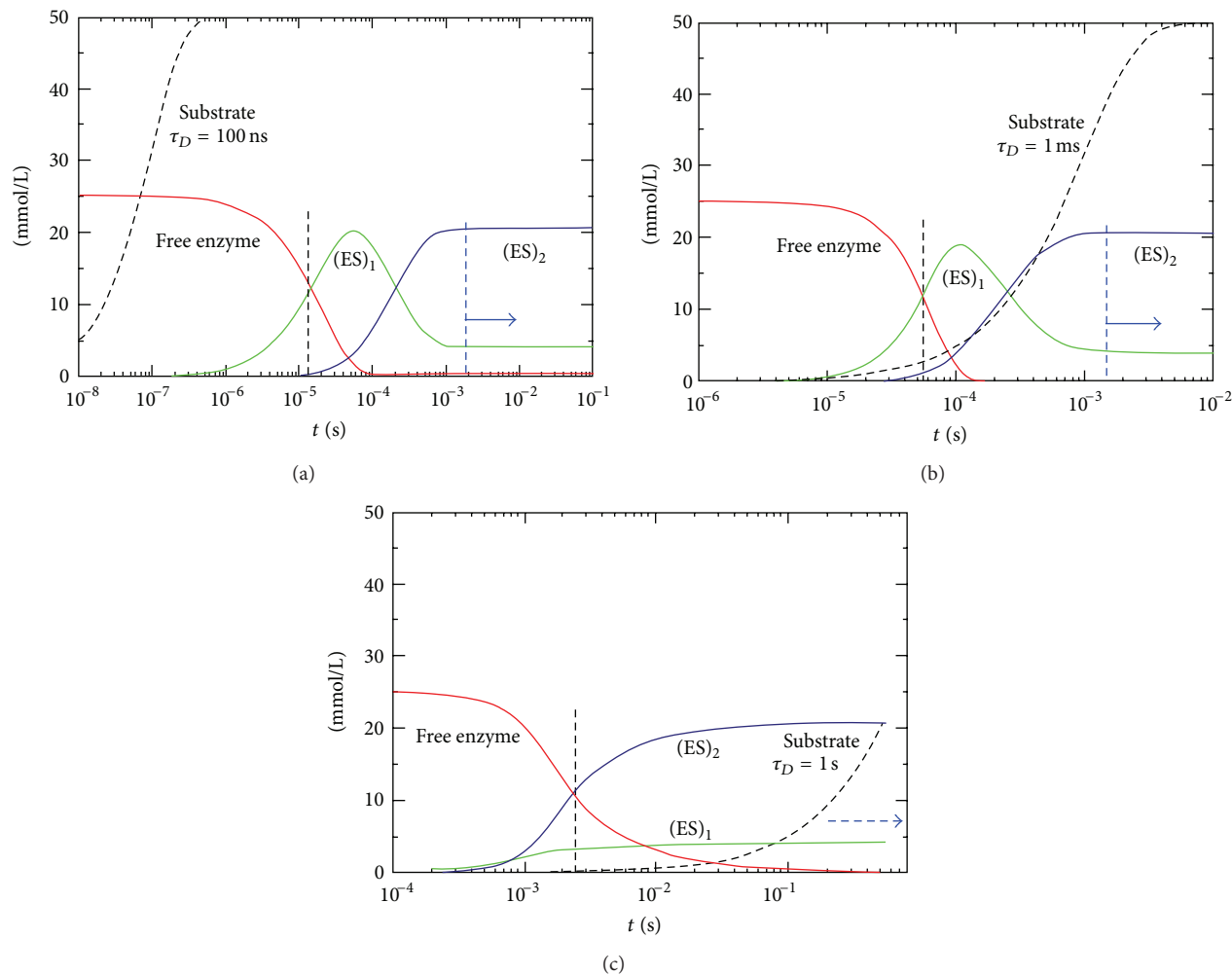


FIGURE 5: Concentration profiles of free enzyme (red),  $(ES)_1$  complex (green), and  $(ES)_2$  complex (light blue); substrate in black. Vertical black dashed lines: relaxation time of the free enzyme, vertical blue dashed lines: beginning of steady state. (a) Caged substrate, activation, and diffusion times much faster than binding, instantaneous activation, (b) mixing, crystal size  $3 \times 4 \times 5 \mu\text{m}^3$ , and diffusion times on the order of the of the turnover time, (c) mixing, crystal size  $100 \times 120 \times 140 \mu\text{m}^3$ , and diffusion time much slower than the turnover time.

magnitude higher than the commonly accepted limit even at cryogenic temperatures, but yet diffraction patterns show no damage [63]. Mix-and-inject transient state kinetic experiments that employ diffusion of substrate into crystals become feasible. Time-resolution is still limited to sub-milliseconds, which is however comparable to using caged substrates. Smaller crystals are also advantageous for pump-probe experiments where reaction is initiated by a femtosecond laser flash (Figure 2(b)). There is only a limited number of photons available in the flash. Since protein crystals are unusually optically thick, only a thin layer of molecules is activated at the surface. If, however, the crystals are very small, the laser flash can initiate a reaction uniformly throughout the entire crystal. For example, photoactive yellow (PYP) protein has a molar absorption coefficient of  $45,500 \text{ cm}^2 \text{ mmol}^{-1}$  at peak absorbance. Given the concentration of  $96 \text{ mmol/L}$  of PYP in the crystal, one absorption unit is reached with  $2.3 \mu\text{m}$  crystals. Unlike larger crystals, the wavelength of the exciting laser can be tuned directly into the absorption maximum ( $449 \text{ nm}$ )

and, still, reaction initiation would be achieved uniformly. Even if the crystal lattice is not commensurable with the macromolecular reaction and the crystal loses integrity at a certain point in time of the reaction, it would still be possible to up to this point in time, because the crystal is discarded in any case and a new one is injected. This holds for both mix-and-inject as well as for pump-probe experiments at the XFEL and potentially, with larger crystals, at the synchrotron. Since the XFEL pulse is quite monochromatic and all the diffraction patterns are stills, all reflections are partials. For each reflection, the intensity is obtained from a sharp intersection of the Ewald sphere with the, in reciprocal space umbrella shaped crystal mosaicity [14] or, for very small crystals, with their shape transforms [36]. This results in an extremely low reflection overlap, even in the presence of higher mosaicity [61]. Consequently, the time-resolved experiment might also work with relatively low quality crystals.

Although some information about the microscopic rate coefficients of the mechanism can be obtained, a

comprehensive mechanism remains underdetermined from only one crystallographic time series. There are more rate coefficients than observables that can be extracted from the time series [64]. An additional parameter such as the temperature can be varied to obtain additional observables. This requires rapid and routine production of entire time series from the beginning to the end of a reaction. With an appropriate design of a mixing device [57] longer time scales become also accessible without sacrificing the advantage of serially providing crystals to the X-ray beam. Before injection, the nanocrystal substrate mixture could reside for an extended period of time within the mixing device's flow, whose velocity can be controlled over a large range to achieve appropriate time delays [57]. When the temperature in the mixing device is also controlled, five-dimensional crystallography [64] becomes possible, and the energetics of the reaction can be investigated in addition. That includes entropy and enthalpy values of the barriers of activation in the chemical, kinetic mechanism. Free energy landscapes of enzymatic reactions become assessable by the time-resolved and temperature-dependent X-ray data.

When mixing times approach diffusion times, it is not very useful to reduce the crystal size further. Given the assumptions in this paper and the best mixers, this limit would be reached approximately with  $0.5\ \mu\text{m}$ – $1\ \mu\text{m}$  sized crystals (see Table 1). The ultimate experiment would be a time-resolved experiment with a “crystal” reduced to the size of a single molecule [65–69]. The substrate would be closely almost instantaneously. The best time-resolution possible is then determined mainly by the mixing time. This suggests that mixers with the fastest mixing times must be available to accommodate such an experiment. Alternatively, caged substrates, which then require appropriate rapid activation rates, can be used in a pump-probe type experiment (Figure 2(b)). To date, no single enzyme molecule was successfully injected into the XFEL beam. The number of photons scattered would be on the order of 200 for a moderately sized enzyme molecule. An extensive number of sparsely populated diffraction patterns must be analyzed with special embedding techniques on an extremely low signal-to-noise level [66, 67]. A small ensemble of single molecules in random orientation may be well prepared in the mixing chamber and injected. There are, indeed, approaches to analyze the diffraction patterns obtained from this ensemble [70, 71]. Angular intensity correlations can be determined from these diffraction patterns [72]. From a large number of correlations, finally, the diffraction volume of a single molecule can be calculated [73]. The time-resolved experiment has the advantage that the structure of the dark or reference state is known, which might be used to facilitate the analysis of these sparse data. However, the experimental and the theoretical framework first have to be implemented and refined (see [74]).

## Acknowledgment

The author thanks Vukica Srajer for critical reading of the paper. The work on time-resolved crystallography is supported by Grant NSF-0952643 (Career), work on the ccNIR

is supported by NSF-1121770, and work on time-resolved structures from solution is supported by NSF-1158138.

## References

- [1] C. O'Sullivan and F. W. Tompson, “LX.—Invertase: a contribution to the history of an enzyme or unorganised ferment,” *Journal of the Chemical Society, Transactions*, vol. 57, pp. 834–931, 1890.
- [2] J. B. Sumner, “The isolation and crystallization of the enzyme urease: preliminary paper,” *The Journal of Biological Chemistry*, vol. 69, pp. 435–441, 1926.
- [3] M. von Laue, *Roentgenstrahlinterferenzen*, Physik und Chemie und ihre Anwendungen in Einzeldarstellungen, Akademische Verlagsgesellschaft, Leipzig, Germany, 1942.
- [4] M. F. Perutz, “Relation between structure and sequence of haemoglobin,” *Nature*, vol. 194, no. 4832, pp. 914–917, 1962.
- [5] J. C. Kendrew, G. Bodo, H. M. Dintzis, R. G. Parrish, H. Wyckoff, and D. C. Phillips, “A three-dimensional model of the myoglobin molecule obtained by X-ray analysis,” *Nature*, vol. 181, no. 4610, pp. 662–666, 1958.
- [6] M. Schmidt, K. Achterhold, V. Prusakov, and F. G. Parak, “Protein dynamics of a  $\beta$ -sheet protein,” *European Biophysics Journal*, vol. 38, no. 5, pp. 687–700, 2009.
- [7] F. G. Parak, K. Achterhold, S. Croci, and M. Schmidt, “A physical picture of protein dynamics and conformational changes,” *Journal of Biological Physics*, vol. 33, no. 5-6, pp. 371–387, 2007.
- [8] K. Moffat, “Time-resolved macromolecular crystallography,” *Annual Review of Biophysics and Biophysical Chemistry*, vol. 18, pp. 309–332, 1989.
- [9] K. Moffat, “Time-resolved biochemical crystallography: a mechanistic perspective,” *Chemical Reviews*, vol. 101, no. 6, pp. 1569–1581, 2001.
- [10] M. Schmidt, S. Rajagopal, Z. Ren, and K. Moffat, “Application of singular value decomposition to the analysis of time-resolved macromolecular X-ray data,” *Biophysical Journal*, vol. 84, no. 3, pp. 2112–2129, 2003.
- [11] M. Schmidt, “Structure based enzyme kinetics by time-resolved X-ray crystallography,” in *Ultrashort Laser Pulses in Medicine and Biology*, W. Zinth, M. Braun, and P. Gilch, Eds., Biological and Medical Physics, Biomedical Engineering, Springer, Berlin, Germany, 2008.
- [12] M. Schmidt, R. Pahl, V. Vukica Srajer et al., “Protein kinetics: structures of intermediates and reaction mechanism from time-resolved X-ray data,” *Proceedings of the National Academy of Sciences of the United States of America*, vol. 101, no. 14, pp. 4799–4804, 2004.
- [13] Z. Ren and K. Moffat, “Quantitative-analysis of synchrotron laue diffraction patterns in macromolecular crystallography,” *Journal of Applied Crystallography*, vol. 28, pp. 461–481, 1995.
- [14] Z. Ren, D. Bourgeois, J. R. Helliwell, K. Moffat, V. Šrajer, and B. L. Stoddard, “Laue crystallography: coming of age,” *Journal of Synchrotron Radiation*, vol. 6, no. 4, pp. 891–917, 1999.
- [15] D. Greiffenberg and A. Collaboration, “The AGIPD detector for the European XFEL,” *Journal of Instrumentation*, vol. 7, 2012.
- [16] H. T. Philipp, M. Hromalik, M. Tate, L. Koerner, and S. M. Gruner, “Pixel array detector for X-ray free electron laser experiments,” *Nuclear Instruments and Methods in Physics Research A*, vol. 649, no. 1, pp. 67–69, 2011.
- [17] H. Graafsma, “Requirements for and development of 2 dimensional X-ray detectors for the European X-ray Free Electron

- Laser in Hamburg,” *Journal of Instrumentation*, vol. 4, no. 12, Article ID P12011, 2009.
- [18] G. Kuriso, A. Sugimoto, Y. Kai, and S. Harada, “A flow cell suitable for time-resolved X-ray crystallography by the Laue method,” *Journal of Applied Crystallography*, vol. 30, no. 1, part 5, pp. 555–556, 1997.
- [19] M. Schmidt, V. Srajer, N. Purwara, and S. Tripathia, “The kinetic dose limit in room-temperature time-resolved macromolecular crystallography,” *Journal of Synchrotron Radiation*, vol. 19, part 2, pp. 264–273, 2012.
- [20] J. E. Knapp, R. Pahl, V. Šrajer, and W. E. Royer, “Allosteric action in real time: time-resolved crystallographic studies of a cooperative dimeric hemoglobin,” *Proceedings of the National Academy of Sciences of the United States of America*, vol. 103, no. 20, pp. 7649–7654, 2006.
- [21] V. Šrajer, T. Y. Teng, T. Ursby et al., “Photolysis of the carbon monoxide complex of myoglobin: nanosecond time-resolved crystallography,” *Science*, vol. 274, no. 5293, pp. 1726–1729, 1996.
- [22] F. Schotte, M. Lim, T. A. Jackson et al., “Watching a protein as it functions with 150-ps time-resolved X-ray crystallography,” *Science*, vol. 300, no. 5627, pp. 1944–1947, 2003.
- [23] J. M. Key, V. Srajer, R. Pahl, and K. Moffat, “Time-resolved crystallographic studies of the heme domain of the oxygen sensor FixL: structural dynamics of ligand rebinding and their relation to signal transduction,” *Biochemistry*, vol. 46, no. 16, pp. 4706–4715, 2004.
- [24] H. Ihee, S. Rajagopal, V. Srajer et al., “Visualizing reaction pathways in photoactive yellow protein from nanoseconds to seconds,” *Proceedings of the National Academy of Sciences of the United States of America*, vol. 102, no. 20, pp. 7145–7150, 2005.
- [25] D. Bourgeois, B. Vallone, A. Arcovito et al., “Extended subnanosecond structural dynamics of myoglobin revealed by Laue crystallography,” *Proceedings of the National Academy of Sciences of the United States of America*, vol. 103, no. 13, pp. 4924–4929, 2006.
- [26] M. Schmidt, K. Nienhaus, R. Pahl et al., “Ligand migration pathway and protein dynamics in myoglobin: a time-resolved crystallographic study on L29W MbCO,” *Proceedings of the National Academy of Sciences of the United States of America*, vol. 102, no. 33, pp. 11704–11709, 2005.
- [27] S. Rajagopal, S. Anderson, V. Srajer, M. Schmidt, R. Pahl, and K. Moffat, “A structural pathway for signaling in the E46Q mutant of photoactive yellow protein,” *Structure*, vol. 13, no. 1, pp. 55–63, 2005.
- [28] S. Tripathi, V. Srajer, N. Purwar, R. Henning, and M. Schmidt, “pH dependence of the photoactive yellow protein photocycle investigated by time-resolved crystallography,” *Biophysical Journal*, vol. 102, no. 2, pp. 325–332, 2012.
- [29] B. Perman, V. Šrajer, Z. Ren et al., “Energy transduction on the nanosecond time scale: early structural events in a xanthopsin photocycle,” *Science*, vol. 279, no. 5358, pp. 1946–1950, 1998.
- [30] F. Schotte, H. S. Cho, V. R. Kaila et al., “Watching a signaling protein function in real time via 100-ps time-resolved Laue crystallography,” *Proceedings of the National Academy of Sciences of the United States of America*, vol. 109, no. 47, pp. 19256–19261, 2012.
- [31] B. L. Stoddard, B. E. Cohen, M. Brubaker, A. D. Mesecar, and D. E. Koshland, “Millisecond laue structures of an enzyme-product complex using photocaged substrate analogs,” *Nature Structural Biology*, vol. 5, no. 10, pp. 891–897, 1998.
- [32] I. Schlichting, J. Berendzen, K. Chu et al., “The catalytic pathway of cytochrome P450cam at atomic resolution,” *Science*, vol. 287, no. 5458, pp. 1615–1622, 2000.
- [33] I. Schlichting, G. Rapp, J. John, A. Wittinghofer, E. F. Pai, and R. S. Goody, “Biochemical and crystallographic characterization of a complex of c-Ha-ras p21 and caged GTP with flash photolysis,” *Proceedings of the National Academy of Sciences of the United States of America*, vol. 86, no. 20, pp. 7687–7690, 1989.
- [34] E. M. H. Duke, S. Wakatsuki, A. Hadfield, and L. N. Johnson, “Laue and monochromatic diffraction studies on catalysis in phosphorylase b crystals,” *Protein Science*, vol. 3, no. 8, pp. 1178–1196, 1994.
- [35] S. Boutet, L. Lomb, G. J. Williams et al. et al., “High-resolution protein structure determination by serial femtosecond crystallography,” *Science*, vol. 337, no. 6092, pp. 362–364, 2012.
- [36] R. A. Kirian, X. Wang, U. Weierstall et al., “Femtosecond protein nanocrystallography—data analysis methods,” *Optics Express*, vol. 18, no. 6, pp. 5713–5723, 2010.
- [37] L. Redecke, K. Nass, D. P. DePonte et al. et al., “Natively inhibited Trypanosoma brucei cathepsin B structure determined by using an X-ray laser,” *Science*, vol. 339, no. 6116, pp. 227–230, 2012.
- [38] R. Koopmann, K. Cupelli, L. Redecke et al. et al., “In vivo protein crystallization opens new routes in structural biology,” *Nature Methods*, vol. 9, no. 3, pp. 259–262, 2012.
- [39] H. N. Chapman, P. Fromme, A. Barty et al., “Femtosecond X-ray protein nanocrystallography,” *Nature*, vol. 470, no. 7332, pp. 73–78, 2011.
- [40] R. Neutze and K. Moffat, “Time-resolved structural studies at synchrotrons and X-ray free electron lasers: opportunities and challenges,” *Current Opinion in Structural Biology*, vol. 22, no. 5, pp. 651–659, 2012.
- [41] S. R. Adams and R. Y. Tsien, “Controlling cell chemistry with caged compounds,” *Annual Review of Physiology*, vol. 55, pp. 755–784, 1993.
- [42] M. Goelder and R. Givens, *Dynamic Studies in Biology: Phototriggers, Photoswitches and Caged Biomolecules*, Wiley VCH, 2005.
- [43] T. Ursby, M. Weik, E. Fioravanti, M. Delarue, M. Goeldner, and D. Bourgeois, “Cryophotolysis of caged compounds: a technique for trapping intermediate states in protein crystals,” *Acta Crystallographica Section D*, vol. 58, no. 4, pp. 607–614, 2002.
- [44] I. Schlichting, S. C. Almo, G. Rapp et al., “Time-resolved X-ray crystallographic study of the conformational change in Ha-Ras p21 protein on GTP hydrolysis,” *Nature*, vol. 345, no. 6273, pp. 309–315, 1990.
- [45] B. L. Stoddard, P. Koenigs, N. Porter, K. Petratos, G. A. Petsko, and D. Ringe, “Observation of the light-triggered binding of pyrone to chymotrypsin by Laue X-ray crystallography,” *Proceedings of the National Academy of Sciences of the United States of America*, vol. 88, no. 13, pp. 5503–5507, 1991.
- [46] E. M. H. Duke, A. Hadfield, S. Walters, S. Wakatsuki, R. K. Bryan, and L. N. Johnson, “Time-resolved diffraction studies on glycogen phosphorylase b,” *Philosophical Transactions of the Royal Society A*, vol. 340, no. 1657, pp. 245–261, 1992.
- [47] A. J. Scheidig, E. F. Pai, I. Schlichting et al., “Time-resolved crystallography on H-ras p21,” *Philosophical Transactions of the Royal Society A*, vol. 340, no. 1657, pp. 263–272, 1992.
- [48] Y. O. Jung, J. H. Lee, J. Kim et al., “Volume-conserving trans-cis isomerization pathways in photoactive yellow protein visualized by picosecond X-ray crystallography,” *Nature Chemistry*, vol. 5, no. 3, pp. 212–220, 2013.
- [49] N. Purwar, J. M. McGarry, J. Kostera, A. A. Pacheco, and M. Schmidt, “Interaction of nitric oxide with catalase: structural

- and kinetic analysis," *Biochemistry*, vol. 50, no. 21, pp. 4491–4503, 2011.
- [50] J. R. Helliwell, Y. P. Nieh, J. Raftery et al., "Time-resolved structures of hydroxymethylbilane synthase (Lys59Gln mutant) as it is loaded with substrate in the crystal determined by Laue diffraction," *Journal of the Chemical Society*, vol. 94, no. 17, pp. 2615–2622, 1998.
- [51] A. Cornish-Bowden, *Fundamentals of Enzyme Kinetics*, Wiley-VCH, 4th edition, 2012.
- [52] M. Youngblut, E. T. Judd, V. Srajer et al., "Laue crystal structure of *Shewanella oneidensis* cytochrome c nitrite reductase from a high-yield expression system," *Journal of Biological Inorganic Chemistry*, vol. 17, no. 4, pp. 647–662, 2012.
- [53] A. V. Cherepanov and S. De Vries, "Microsecond freeze-hyperquenching: development of a new ultrafast micro-mixing and sampling technology and application to enzyme catalysis," *Biochimica et Biophysica Acta*, vol. 1656, no. 1, pp. 1–31, 2004.
- [54] D. P. Deponte, J. T. Mckeown, U. Weierstall, R. B. Doak, and J. C. H. Spence, "Towards ETEM serial crystallography: electron diffraction from liquid jets," *Ultramicroscopy*, vol. 111, no. 7, pp. 824–827, 2011.
- [55] A. M. Gañán-Calvo, D. P. DePonte, M. A. Herrada, J. C. H. Spence, U. Weierstall, and R. B. Doak, "Liquid capillary micro/nanojets in free-jet expansion," *Small*, vol. 6, no. 7, pp. 822–824, 2010.
- [56] R. G. Sierra, H. Laksmono, J. Kern et al. et al., "Nanoflow electrospinning serial femtosecond crystallography," *Acta Crystallographica D*, vol. 68, no. part 11, pp. 1584–1587, 2012.
- [57] H. Y. Park, X. Qiu, E. Rhoades et al., "Achieving uniform mixing in a microfluidic device: hydrodynamic focusing prior to mixing," *Analytical Chemistry*, vol. 78, no. 13, pp. 4465–4473, 2006.
- [58] H. S. Carslaw and J. C. Jaeger, *Conduction Heat in Solids*, Clarendon Press, Oxford, UK, 2nd edition, 1959.
- [59] J. Hajdu, K. R. Acharya, D. I. Stuart et al., "Catalysis in the crystal: synchrotron radiation studies with glycogen phosphorylase b," *EMBO Journal*, vol. 6, no. 2, pp. 539–546, 1987.
- [60] S. Geremia, M. Campagnolo, N. Demitri, and L. N. Johnson, "Simulation of diffusion time of small molecules in protein crystals," *Structure*, vol. 14, no. 3, pp. 393–400, 2006.
- [61] A. Aquila, M. S. Hunter, R. B. Doak et al. et al., "Time-resolved protein nanocrystallography using an X-ray free-electron laser," *Optics Express*, vol. 20, no. 3, pp. 2706–2716, 2012.
- [62] J. M. Holton and K. A. Frankel, "The minimum crystal size needed for a complete diffraction data set," *Acta Crystallographica Section D*, vol. 66, no. 4, pp. 393–408, 2010.
- [63] L. Lomb, T. R. M. Barends, S. Kassemeyer et al., "Radiation damage in protein serial femtosecond crystallography using an X-ray free-electron laser," *Physical Review B*, vol. 84, no. 21, Article ID 214111, 2011.
- [64] M. Schmidt, T. Graber, R. Henning, and V. Srajer, "Five-dimensional crystallography," *Acta Crystallographica A*, vol. 66, part 2, pp. 198–206, 2010.
- [65] R. Neutze, R. Wouts, D. Van Der Spoel, E. Weckert, and J. Hajdu, "Potential for biomolecular imaging with femtosecond X-ray pulses," *Nature*, vol. 406, no. 6797, pp. 752–757, 2000.
- [66] D. Giannakis, P. Schwander, and A. Ourmazd, "The symmetries of image formation by scattering. I. Theoretical framework," *Optics Express*, vol. 20, no. 12, pp. 12799–12826, 2012.
- [67] P. Schwander, C. H. Yoon, A. Ourmazd, and D. Giannakis, "The symmetries of image formation by scattering. II. Applications," *Optics Express*, vol. 20, no. 12, pp. 12827–12849, 2012.
- [68] R. Fung, V. Shneerson, D. K. Saldin, and A. Ourmazd, "Structure from fleeting illumination of faint spinning objects in flight," *Nature Physics*, vol. 5, no. 1, pp. 64–67, 2009.
- [69] M. M. Seibert, T. Ekeberg, F. R. N. C. Maia et al., "Single mimivirus particles intercepted and imaged with an X-ray laser," *Nature*, vol. 470, no. 7332, pp. 78–82, 2011.
- [70] D. K. Saldin, V. L. Shneerson, M. R. Howells et al., "Structure of a single particle from scattering by many particles randomly oriented about an axis: toward structure solution without crystallization?" *New Journal of Physics*, vol. 12, Article ID 035014, 2010.
- [71] D. K. Saldin, H. C. Poon, P. Schwander, M. Uddin, and M. Schmidt, "Reconstructing an icosahedral virus from single-particle diffraction experiments," *Optics Express*, vol. 19, no. 18, pp. 17318–17335, 2011.
- [72] R. A. Kirian, K. E. Schmidt, X. Wang, R. B. Doak, and J. C. H. Spence, "Signal, noise, and resolution in correlated fluctuations from snapshot small-angle X-ray scattering," *Physical Review E*, vol. 84, no. 1, part 1, Article ID 011921, 2011.
- [73] D. K. Saldin, H. C. Poon, V. L. Shneerson et al., "Beyond small-angle X-ray scattering: exploiting angular correlations," *Physical Review B*, vol. 81, no. 17, Article ID 174105, 2010.
- [74] H. C. Poon, M. Schmidt, and D. K. Saldin, "Extraction of fast changes in the structure of a disordered ensemble of photoexcited biomolecules," *Advances on Condensed Matter Physics*. In press.

